Residual stress in machined duplex stainless steel welds developed through automatic process

Payares-Asprino, Carolina; Munoz de Escalona, Patricia; Sanchez, Ana

Published in:
IV International Conference on Welding and Joining of Materials - ICONWELD 2018

Publication date:
2019

Document Version
Author accepted manuscript

Residual Stress in Machined Duplex Stainless Steel Welds Developed through Automatic Process.

Carolina Payares-Asprino[1, a], Patricia Muñoz-Escalona[2, b], Ana Sanchez[3, c]

[1]Norwich University, Mechanical Engineering Dept., 158 Harmon Drive, Northfield, Vermont 05663, USA

[2]Glasgow Caledonian University, School of Engineering and Built Environment, Glasgow, G4 0BA, UK.

[3]CIATEQ, Centro Tecnológico Avanzado, Av. del Retablo 150 Col. Querétaro, México

[a]mpayares@norwich.edu, [b]patricia.munoz@gcu.ac.uk, [c]anamelis.sanchez@utng.edu.mx

Abstract

As design engineering components have become less conservative, there has been an increase interest in the effect of residual stresses on mechanical properties. The demand for high quality focuses attention on product's surface integrity such as residual stresses in the weld's machined surface due to their effect on product's performance, longevity and reliability (e.g. joining process of pipes which usually includes welding and surface machining). Both processes (welding and machining) induce residual stresses which end-up with the occurrence of stress corrosion cracking. It is therefore necessary to quantify the material's integrity properties of the weld bead as a function of the machining conditions. The aim of this research is focus on the analysis of the residual stresses developed as a consequence of a welding process and subsequent machining of the weld bead conducted on duplex stainless steel. Two main variables were studied: i) heat input as a welding variable and ii) chips cross-sectional area as a machining variable.

The residual stress was measured in all samples after the welding process and after the machining of the weld bead. These measurements were conducted using the Hole-Drilling strain-gage technique. Results showed that higher values of compressive residual stresses were generated when developing chips with a cross-sectional area of 0.3 mm^2, and that the tensile residual stresses increased in the weld bead when machining the weld beads with constant chip cross-sectional area of 0.6 mm^2.

1. Introduction

Effective weld design can produce physical and mechanical properties within the weld bead which approach those of the base metal. The mechanical properties of a welded material depend on the resulted microstructure as a consequence of the phase transformation characteristics which are governed by the continuous-cooling transformation (CCT) behavior. The heating and cooling rate, determined by the welding conditions (welding technique, arc current, arc voltage, welding speed, and heat input), are responsible for the temperature-time cycle at each point of the fusion zone and heat affected zone of the weld. Hence, it is extremely important to study the effect of heat input on the value and distribution of the residual stresses in the weld, where the peak stress occurs in the center of the weld bead just where the yield stress is higher [1]

Duplex stainless steels (DSS) are widely used in many engineering applications such as those found in the petrochemical, pulp and paper, and oil and gas industries, since they exhibit good mechanical properties and high corrosion resistance. Properties such as high tensile strength, high fatigue strength, good toughness even at low temperature, adequate formability and weldability and excellent corrosion resistance (e.g. stress corrosion cracking and pitting) result from the almost equal amount of ferrite (α) phase and austenite (γ) phase present in this steel. The presences of these two phases combine the attractive properties of austenitic and ferritic steels: [2-4]. There is an increase used of DSS in the pipe industry compared to austenitic stainless steels, particularly where chloride or sulphide stress corrosion cracking is of primary concern [5]. However, the solidification of duplex stainless steel welds does not always produce near equal amounts of ferritic (α) and austenitic (γ) phase, as occurs in the parent metal; thus deteriorating the mechanical properties and corrosion resistance of the weld joint. The microstructures developed in the weld's fusion zone and the heat-affected zone (HAZ) also have a significant influence on the mechanical properties and corrosion resistance of duplex stainless steels [6]

In welded structures, the inevitable existence of residual stresses is well known, as these are produced as a result of the plastic deformation caused by non-uniform thermal expansion and contraction imposed during the process. The residual stresses are always self-equilibrated and the magnitude of tensile residual stresses within and near the weld area are high enough to have deleterious effects on the structural integrity of the welded joints, increasing the susceptibility to fatigue damage, stress corrosion cracking and brittle fracture [5]. These stresses when combined with applied stresses can reduce material's fatigue life and accelerate growth rates of pre- existing or service-induced defects on structural systems. Therefore knowledge of the magnitude and the distribution of the residual stresses will help on the production of an efficient and economic design as well as on the good performance of the mechanical structures. However, accurate prediction of welding residual stresses is very difficult due to the complexity of the process which involves localized heating, temperature dependence of material properties and movement of the heat source, etc.

In general, the machining of stainless steels is different when compared with other steels, since it is mainly characterized by high strain rates that induce mechanical properties modifications and a heterogeneous behavior on the developed surface due to the generation of an unstable chip formation and vibrations [7]. Previous research has shown that stainless steels microstructure has got a bigger effect on the machining process compared to the effect of the material's hardness; an example of this was investigated by Bletton et al. [8], where it was mentioned that the two-phase structure of the duplex stainless steels, contribute to induce vibrations during the machining process, increasing the problems previously mentioned and contributing to the decrease of tool life. The difficulties in the machining process tend to increase when using super duplex stainless steel due to the presence of austenite, nitrogen and alloying elements, therefore the machining of this material is frequently compared with its PRE (Pitting Resistance Equivalent) [9]. Another factor that contributes to the difficulties in the machining process of super duplex stainless steel is the fact that that this material is biphasic and each phase is not only randomly distributed, but also contains different characteristics and properties, where each of them contributes in a different way to the chip formation and the cutting process in general. The demand of high

quality products has focused its attention on the residual stress of the machined surfaces, due to its effect on the component's longevity and reliability [7, 10]. Many structural failures produced by fatigue, creep and stress corrosion cracking, are initiated on the component's machined surface, therefore it is of extreme importance to characterize the influence of the machining conditions on the workpiece's surface [11]. Cai et al. [12] studied the effect of high speed end milling on the surface integrity of 7075 aluminum alloy. Their results showed that a high cutting speed has a positive effect on the surface finish, and that residual stresses will be transformed from tensile values to compressive values when the cutting speed is increased. The initiation and propagation of stress corrosion cracking (SCC) is a result of the superposition effect of sensitization due to the temperature history of the welds, the corrosive atmosphere and the residual stress due to the welding process. Low-carbon austenitic type 316L stainless steel was developed to reduce the effect of sensitization; nevertheless, SCC was observed near the weld zone of the core shroud and primary loop recirculation (PLR) [13].

Surface machining is usually conducted before and after the butt welding of pipes in order to match the inside pipe diameters and to provide a smooth surface finish, where the residual stresses are induced by both processes, (welding and machining), and are an important factor in the initiation and propagation of SCC [14]. Ihara et al. [15] studied the effect of residual stress distributions due to surface machining and welding on low carbon austenitic stainless steel type 316L. The analysis showed that tensile residual stress due to surface machining only exists approximately 0.2mm underneath the machined surface, and that surface residual stress increased when increasing the cutting speed. The crack growth analysis showed that the crack depth is affected by the surface machining and the welding processes, and the crack length is more affected by surface machining than by the welding process. Li et al. [16] found that the solid-state phase transformation has a significant influence on the formation of welding residual stress on P92 steel. The peak temperature of final thermal cycle can determine the magnitude of final stress. Fatigue strength were improved when steel wires were capable of inducing an overall compressive residual stress. It was concluded that the higher compressive residual stresses resulted in improved fatigue properties [17].

2. Experimental Procedure

2.1 Workpiece Characteristics

Duplex Stainless Steel SAF 2205 was selected as parent material as it is widely used in the petrochemical industry. Table 1 shows the chemical composition of SAF 2205 DSS and filler metal ER-2209 which is recommended by ASTM 4815 and A789 procedures for submerged arc welding process (SAW). This ER 2209 - 22.8.3.L electrode wire had 2.4 mm diameter [17]. The welds were produced using a Lincoln Electric, model NA-3S, using DC. Sandvik 15W welding flux was used. The mechanical properties of the parent material are given in Table 2.

Table 1. Chemical composition of the DSS SAF 2205 plate and the ER 2209 electrode (mass,%)

Material	C	Cr	N	Mo	Cu	Si	Mn
SAF 2205	0.045	20.37	5.31	5.31	0.15	0.36	1.41
ER-2209	0.015	25.97	9.81	3.72	0.18	0.67	1.17

Table 2. Material Properties of the SAF 2205

Yield Stress (MPa)	Tensile Stress (MPa)	Elongation (%)	Young's Modulus (GPa)	Poisson's ratio
731	824	15.8	200	0.3

2.2 Welding Parameter.

Single bead-on-plate welds were developed using SAW on DSS plates under different welding conditions. Equation 1 was used for heat input calculations, where recommended values range between 0.5 and 2.5 kJ/mm for stainless steel duplex SAF 2205 [18]. The bead-on-plate (BOP) welds were produced using the conditions shown in Table 3. For the Design of Experiments the Taguchi Method was applied with a L_9, matrix (3 factors: arc current, arc voltage and welding speed at 3 levels each (low, medium and high). Figure 1 shows a schematic drawing of the BOP welds and dimensions of the plate.

$$HI\ (Heat\ input) = \frac{Arc\ current\ x\ Arc\ voltage\ x\ 60}{Welding\ speed\ x\ 1000} \quad (1)$$

Where

$HI\ (kJ/mm), Arc\ Voltage\ (V), Arc\ Current\ (A), Welding\ speed\ (mm/min)$.

Table 3. Selected welding parameters

	Levels		
Factor	**1**	**2**	**3**
Arc Current (A)	300	350	450
Arc Voltage (V)	28	30	32
Welding Speed, WS (mm/min)	576	630	1008

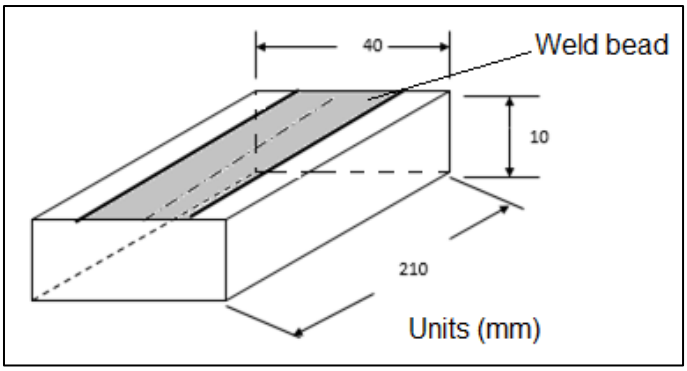

Figure 1. Schematic drawing of the Bead on Plate (BOP) welds

2.3 Cutting Parameters.

The cutting parameters selected for this study were the cutting speed (Vc), the feed per tooth (fz), and the depth of cut (ap), since from limited previous research it was observed that these variables had most influence on the residual stress [12,15]. Selected cutting parameters were recommended from the manufacturer for the parent metal and are shown in Table 4. [19]. For the machining of the weld beads the Taguchi method was also applied, in this case a L_{27} matrix was used. A Fadal CNC milling equipment model MC 3016, with a maximum spindle of 10,000 rpm was used for the face milling operation of the welds.

Table 4. Selected Cutting Parameters

	Levels		
Factor	**1**	**2**	**3**
Vc (m/min)	100	130	160
fz (mm/rev*tooth)	0.1	0.2	0.3
ap (mm)	1.0	1.5	2.5

2.4 Measurements of residual stress.

Residual stress was measured after the welding process and after machining the weld bead. Measurements were conducted using the incremental hole-drilling (HD) technique and following ASTM E837-08 standard [20]. Three - grids strain gauge rosettes (CEA-06-062UM-120, CEA-06-062UL-12) was attached on the HAZ of the welded surface, with a radius of the gage circle (r) of 2.565 mm. The radius of the drilled hole is 0.75 mm. Measurements were recorded every 0.1 mm in depth until reaching a maximum depth of 0.8 mm from the machined surface. Hole-Drilling residual stresses calculations Program software (version 3.21) was used to convert the strain values into residual stress values

The maximum and minimum principal residual stress were calculated using Eq.(2)

$$\sigma_{max,}\sigma_{min} = \frac{\varepsilon_1 + \varepsilon_2}{4A} - \frac{1}{4B}\sqrt{(\varepsilon_3 - \varepsilon_1)^2 + (\varepsilon_3 + \varepsilon_1 - 2\varepsilon_2)^2} \tag{2}$$

$$A = -\frac{1+v}{2E}\left(\frac{1}{r^2}\right) \qquad B = -\frac{1+v}{2E}\left[\left(\frac{4}{1+v}\right)\frac{1}{r^2} - \frac{3}{r^4}\right] \qquad \tan 2\alpha = \frac{\varepsilon_1 - 2\varepsilon_2 + \varepsilon_3}{\varepsilon_1 - \varepsilon_3}$$

where, A and B are calibration coefficients; E=200 GPa, is the Young's modulus of SAF 2205 steel at ambient temperature; v=0.3 is the Poisson's ratio; α is the angle measured clockwise from gage 1 to the nearby principal stress direction, r is the gage circle and $\varepsilon_1, \varepsilon_2, \varepsilon_3$ correspond to the measured relieved strains in three directions.

The maximum and minimum principal stresses can also be calculated using Eq. (3) where the calibration constants $\bar{a}$ and $\bar{b}$ are available and depend on the material.

$$\sigma_{max},\sigma_{min} = E\left[-\frac{\varepsilon_{3+}\varepsilon_1}{2\,\bar{a}\,(1+v)} \pm \frac{\varepsilon_{3+}\varepsilon_2}{2\,\bar{b}}\right] \quad (3)$$

$$\bar{a} = -\frac{2E\bar{A}}{1+v} \qquad \bar{b} = -2E\bar{B}$$

Since, Eq.(2) does not allow to calculate the residual stress as single value, Eq. (4) was used combining $\sigma_{max}, \sigma_{min}$ where one value of residual stress was calculated for each experiment [21].

$$\sigma = (\sigma_{max} + \sigma_{min})\bar{A} + (\sigma_{max} - \sigma_{min})\bar{B}cos2\beta \quad (4)$$

where β is the angle from the x axis to the direction to the maximum principal stress σ_{max}. It must be highlighted that the residual stresses were measured on HAZ after the welding process and after the machining of the weld bead.

Figures 2a. and 2b. shows a schematic drawing of strain gages location in welding heat affected zone and machined weld bead respectively. Figure 2c. shows strain gage.

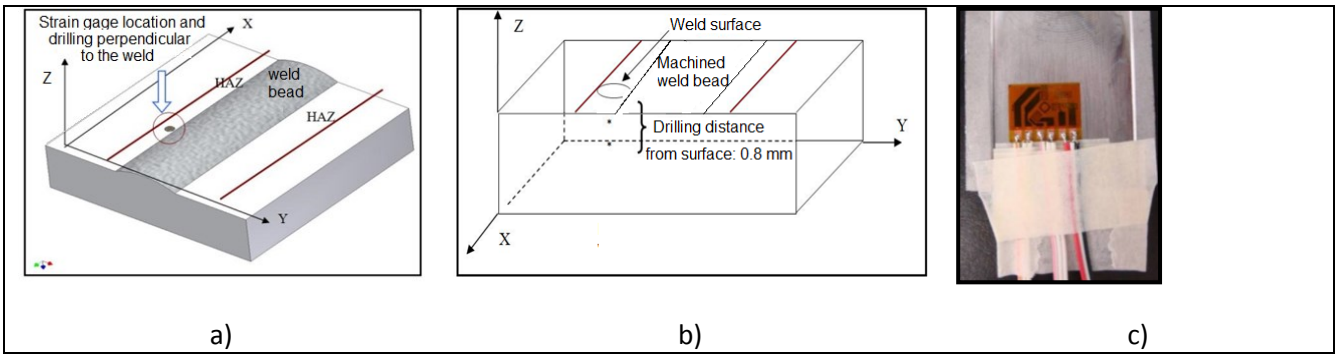

Figure 2. Location of strain gages in a) Weld HAZ, b) Machined Weld Bead and c) CEA-06-062UL-12 strain gage installation.

3. Results and discussions

3.1 Effect of Heat Input on Residual Stress of DSS Heat Affected Zone

Figure 3 show the behavior of residual stress along the drilling distance from HAZ weld surface to 0.8 mm in depth for different heat inputs a) 0.5 kJ/mm, b) 0.86 kJ/mm and c) 1.37 kJ/mm respectively. When analyzing this figure it can be observed that in general the presence of residual stress were more noticeable from 0.2 mm in depth from the weld surface, independently of the value of heat input. In all cases the peak value of residual stress started to appear after 0.5 mm from the weld surface with a maximum value of ~260MPa in tensile stress for all cases. A clear tendency for tensile stress distribution as an effect of the heat input was not obtained. However it was noticed that an average increase of 65% of the heat input produced an increase of 30% in average of the tensile stress. This is probably due

to the welding deformation which occurs under the more extensive thermal excursion. As previously mentioned high attention must be conducted to this result as high tensile residual stresses near the weld bead deteriorate fatigue properties of the weld joint [17,23].

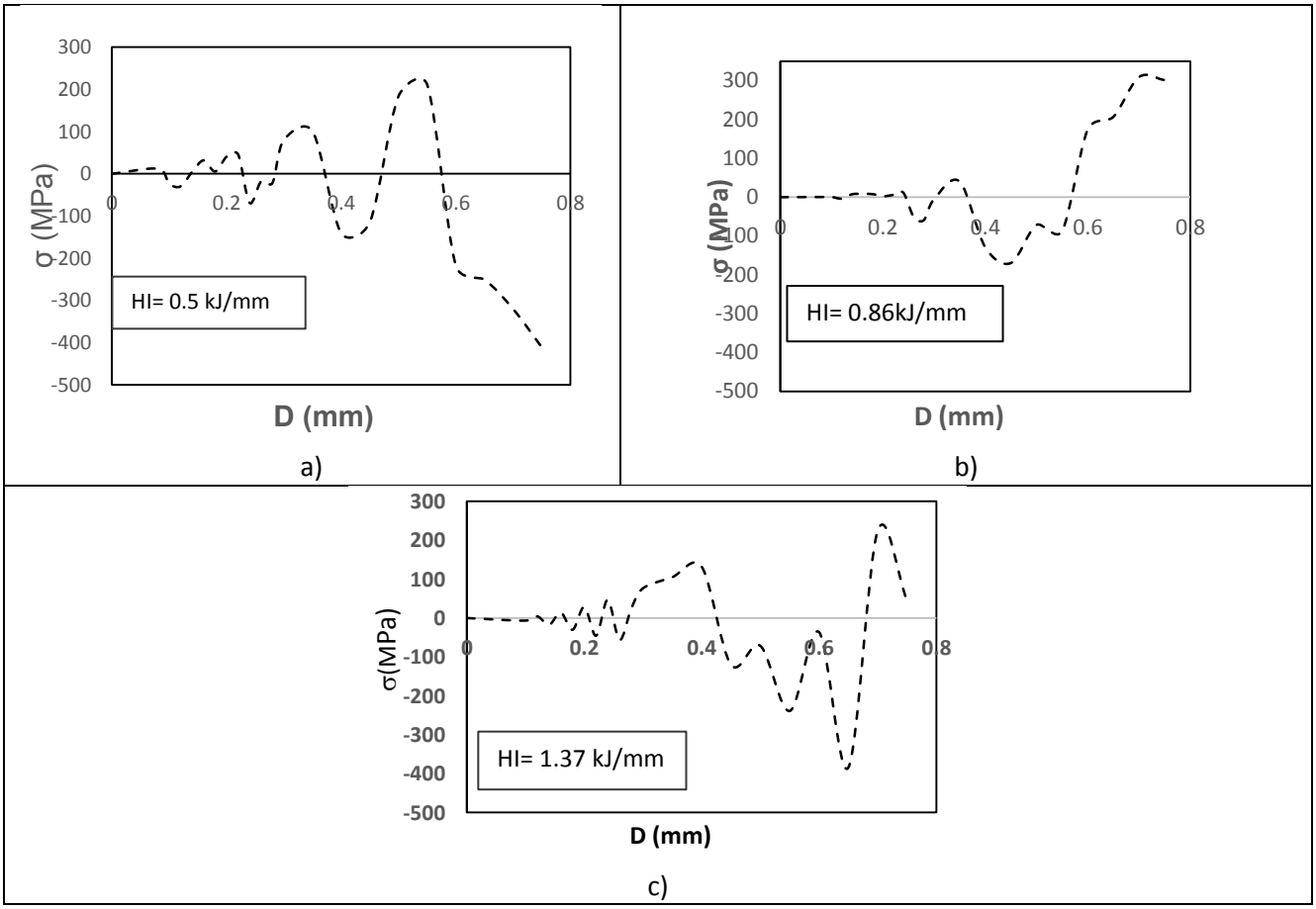

Figure 3. Residual Stress vs drilling distance from Weld Surface (D), measured for a)0.5 kJ/mm, b)0.86 kJ/mm and c)1.37 kJ/mm

3.2 Effect of chip's cross sectional area on Residual Stress of DSS welds.

As previously mentioned the parameters established to determine the behavior of residual stresses in the machining process of welding stainless steel SAF 2205, were the heat input and chips cross-sectional area $(av = ap \cdot fz)$. Figures 4 and 5 show the behavior of the residual stresses below the weld machined surface up to a distance of 0.8 mm for heat inputs of 0.5kJ/mm and 0.86kJ/mm respectively. Results show that independently of the heat input, when machining weld beads at a constant chip's cross-sectional area of 0.3 mm^2 no tensile stresses were generated along the selected distance (see Fig 4a. and Fig 5a), however situation changed when increasing the chip's cross-sectional area in 100% (from 0.3 mm^2 to 0.6 mm^2) where an increase in tensile stress is observed closer to the weld surface with maximum values reported between 0.1-0.3 mm below the surface. These results agree with Cai et al.[12] and Paolinelli [21], where they established that when removing small amount of material during a cutting process, tensile residual stress can be reduced avoiding the appearance of cracks and improving material's structural integrity and resistance to fatigue life. When

the compressive residual stress exists, residual stress could be beneficial as it could relieve the stress concentration effect caused by the applied load [24].

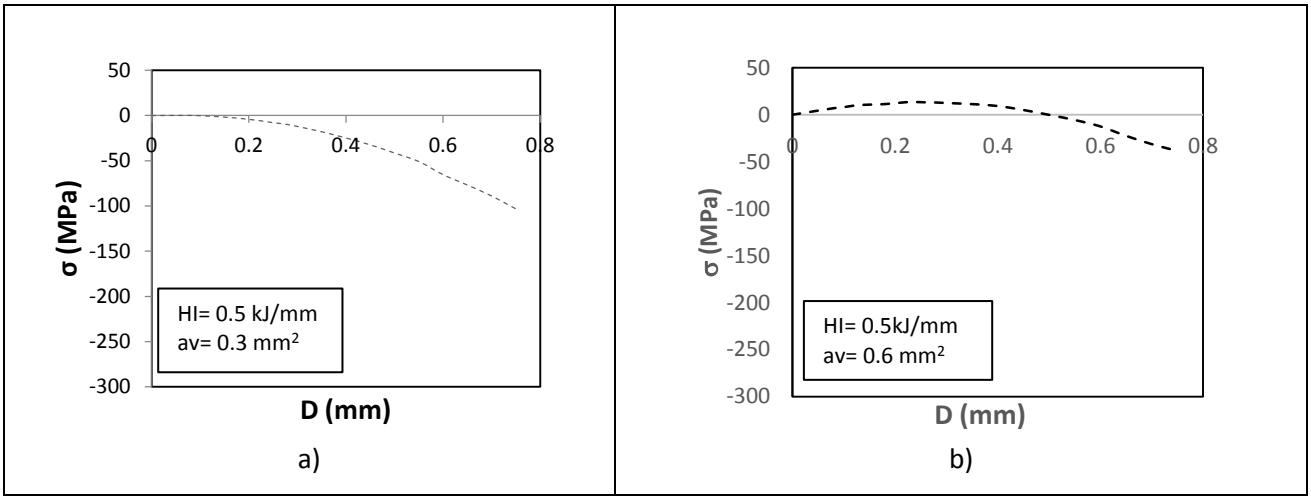

Figure 4. Residual Stress versus drilling distance from Weld Surface (D), measured, for HI = 0.5 kJ/mm: a) chip cross-sectional area, av= 0.3 mm² and b) chip cross-sectional area, av= 0.6 mm²

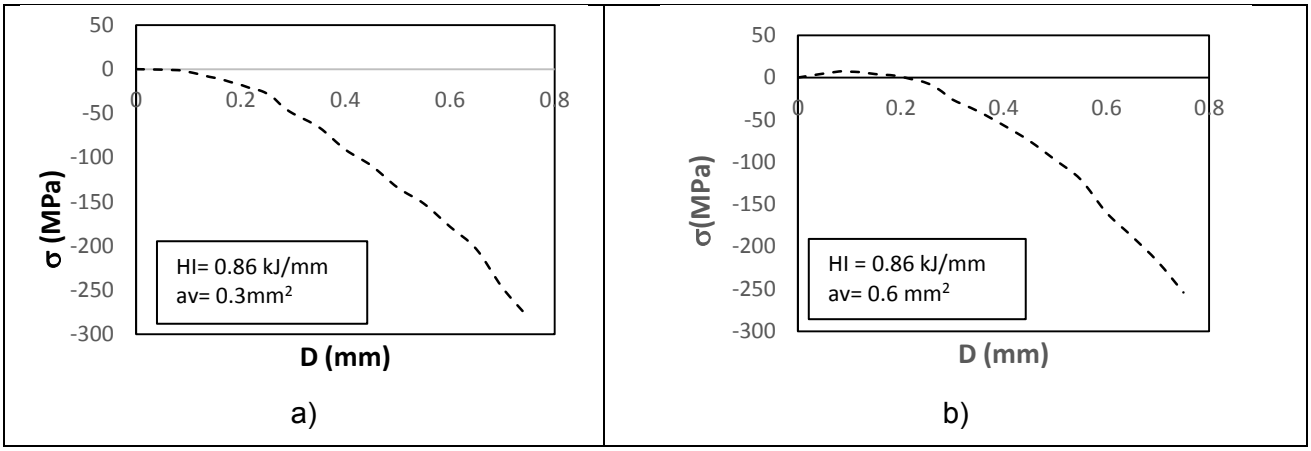

Figure 5. Residual Stress versus drilling distance of Weld Surface, measured for HI= 0.86 0.5 kJ/mm: a) chip cross-sectional area, av= 0.3 mm² and b) chip cross-sectional area, av= 0.6 mm²

4. Conclusions

- An increase in the heat input produces an increase in the welding deformation leading to an increase of the residual stress.
- Higher compressive stress were produced when weld beads were machined using a constant chip cross-sectional area of 0.6 mm² reaching a maximum value of ~ -295MPa

- Independently of the heat input non tensile stresses were developed when machining at constant chip cross-sectional area of 0.3 mm^2 (small amount of material removal)
- Tensile stresses were generated when weld bead was machined using a constant chip cross-sectional area of 0.6 mm^2.
- Taguchi method has shown to be an excellent Design of Experiment approach as optimizes the number of experiments representing savings in time and costs.

5. References

[1] A.M. Paradowska. J.W.H. Price., Journal of Achiev. in Mater. And Manufact. Eng. Vol. 17. issue 1-2, pp. 385-388, 2006.

[2] A.-A. Iris, , Recent Pat. Mech. Eng. Vol.1 pp. 51- 57, 2008.

[3] J.J. del Coz Díaz, P. Menendez Rodriguez, P.J. Garcia Nieto, D. Castro- Fresno, Appl. Therm. Eng., Vol. 30, pp. 2448-2459, 2010.

[4] A.-H.I. Mourad, A. Khourshid, T. Sharef, Mater. Sci.Eng. Vol. A 549, pp.105-113, 2012.

[5] C-H. Lee, K-Ho Chang, Appl. Therm. Eng., Vol. 63, pp. 140-150, 2014.

[6] Payares-Asprino,C**.,** Evans R., Liu, S,Soldagem e Inspecção ,Vol.13 (2),150-159**,** 2008.

[7] R. M Saoubi, J. C., Outeiro, B. Changeux, J. L. Lebrun and A. M., Dias, Journal of Mater. Process. Techn., Vol.96, pp. 225-233, 1999.

[8] O. Bletton, R. Duet and B. Heritier, in Usinabilité des aciers inoxydables. Edited by P. Lacombe, B. Baroux and G.Beranger, Les Aciers Inoxydables, Les Editions de Physique, chap.21, pp. 759-794, 1990.

[9] L. Jiang, J. Paro, H. Hänninen, V. Kauppinen, and R. Oraskari, Journal Mater Process. Techn., Vol.62, pp. 1-9, 1996.

[10] D. Y. Jang, T.R. Watkins, K.J. Kozaczek, C.R. Hubbard, and O.B. Cavin, O. B., Wear, Vol.194, pp. 168-173, 1996.

[11] X. Sauvage, J.M. Le Breton, A. Guillet, A. Meyer and J. Teillet, Mater. Sci. ang Eng. Vol. A362, pp. 181-186, 2003.

[12] X. J. Cai, W.W. Ming and M. Chen, Adv. Mater. Res*.,* Vol. 426. pp. 321–324, 2012

[13] Y. Okamura, A. Sakashita, T. Fukuda, H. Yamashita, and T. Futami, Transac. on SMIRT Vol. 17, No. WG01-1,2003.

[14] K. Takamori, S. Suzuki, S. Ooki, H. Yamashita, T. Tsuneo, H. Anzai, T. Kato,Y Saito. and M. Tsubota, High Pressure Institute of Japan Vol.44 (3), 130–142, 2006.

[15] R. Ihara, J. Katsuyama, K. Onizawa, T Hashimoto, Y. Mikami, and M. Mochizuky. Nuclear Eng. And Design, Vol 241, pp 1335-1344, 2011.

[16] S. Li, S. Ren, Y. Zhang, D. Deng, and H. Murakawa. Ournla of Mater. Process. Technol., Vol. 244, pp. 240-252, 2017.

[17] Darcis, P., Katsumoto, H., Payares-Asprino, M.C**.,** .Liu.,S., Siewert*,*T.A. . Fatigue, Fracture, Eng. Mat. Structure, Vol. 1, pp.1-12, 2007.

[18] Payares-Asprino, M.C., Muñoz-Escalona, P. Sanchez, A. Residual Stress Analysis in Machining of Duplex Welds, AWS Conference held in Chicago, USA, November 2011

[19] Sandvik Coromant, in *Modern machining, practical manual*, edited by Department of technical editions of the company Sandvik Coromant. pp172-173, 2017.

[20] ASTM. E837 -01. Standard test method for determining residual stresses by the hole drilling strain gage method, 2008.

[21] Withers P.J. and Bhadeshia H. K. D. H. Mater. Sci. Techn.Vol. 17, pp.355-365, 2001
[22] Paolinelli L.D. Echeverría M.D.,Jornadas Sam. Conamet, Argentina,. pp 22-27., 2003
[23] Zhongyin, Z. , Peng, C., Hongmei, Z., Yonghui,Z., Yonghong,C., Hao, X., and Aiqin,T., Trans. Tech. Publications Switzerland, Vol. 337, pp. 255-261, 2011.
[24] Jiang,J., Mingshan, Z., Journal of Constructional Steel Research, ol.72, pp.20-28, 2012.
.